Improved Synchronization Scheme for the Photon-Counting-Based Underwater Optical Wireless Communication System

Nuo Huang , Yu Zhu , Weijie Liu , and Zhengyuan Xu , *Senior Member, IEEE*

Abstract—To address existing issues in conventional correlation method, we propose an improved synchronization method for photon-counting-based underwater optical wireless communication system employing on-off keying modulation.The proposed method jointly estimates the synchronization position, signal intensity, background intensity and data sequence based on the received vector in the period of a frame length. To reduce the complexity for solving the estimation problem, several simplifications are performed based on the characteristics of the data sequence. Experimental results show that the proposed method achieves an optical power gain of at least 1 dB over the correlation method at the bit error rate of 10^{-3} under dynamic channel.

Index Terms—Photon-counting, underwater optical wireless communication, synchronization.

I. INTRODUCTION

DUE to the important role in ocean exploration, underwater wireless communication has drawn extensive attentions in recent years [1]. Radio frequency (RF) communication cannot support long transmission distance in the water due to the high attenuation, while acoustic communication suffers low data rate and intolerable transmission latency [2], [3]. Compared with RF communication and acoustic communication, underwater optical wireless communication (UOWC) can achieve higher data rate with lower latency [4]. A UOWC system typically adopts light-emitting diode (LED) or laser diode as the transmitter, and intensity detector or photon-counting detector as the receiver [5], [6]. Under strong received light, the intensity detector such as photodiode can be employed to output continuous waveform whose sampled values can be modeled by a Gaussian distribution. Under weak received light, the photon-counting detector such as photomultiplier tube (PMT) is employed to realize photon-level signal reception [7], [8], [9], where the number of received photons can be characterized by a Poisson distribution [10].

Synchronization is an important part in UOWC. For UOWC systems with intensity detector, there have been plenty of studies on synchronization [11]. However, for UOWC system with photon-counting detector, there are only a few works on synchronization. In [12], a correlation-based synchronization method was proposed for the photon-counting based system, which divides the received signal into small chips and estimates the position of the sync word by maximizing the correlation value between the sync word and the number of received photons within the synchronization window. Despite the implementation simplicity, the correlation-based method neglects the signals surrounding the sync word and thus leads to a transmission performance degradation. Meanwhile, some unfavorable factors (e.g., bubble and turbulence) in real underwater scenarios can cause drastic fluctuation of the optical link, bringing challenges to synchronization in photon-counting-based UOWC systems [13].

To address the above issues, we propose an improved synchronization method for photon-counting-based UOWC system employing on-off keying (OOK) modulation. The proposed method jointly estimates the synchronization position, signal intensity, background intensity and data sequence based on the received vector in the period of a frame length. To reduce the complexity for solving the estimation problem, several simplifications are performed using the characteristics of the data sequence. Experimental results verify the performance improvement by the proposed method over the correlation method. The performance superiority makes the proposed method appealing in real applications.

II. SYSTEM MODEL

Consider a photon-counting-based UOWC system adopting a blue/green LED at the transmitter and a photon-counting detector (e.g., PMT) at the receiver. Non-return-to-zero-OOK modulation is employed for its simplicity. As in Refs. [14], [15], [16], authors assume that the data is transmitted in successive frames with frame length N, as illustrated in Fig. 1. Each frame consists of an L-length fixed sync word and an $(N - L)$-length random data sequence.

To realize synchronization, we consider the received signals in N successive symbol durations and divide each symbol duration
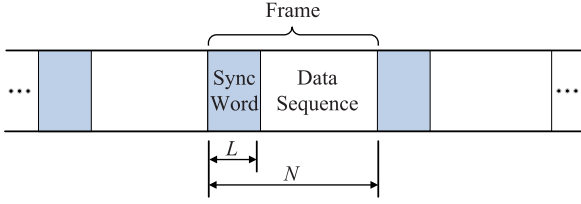
Fig. 1. Illustration of the considered frame structure.
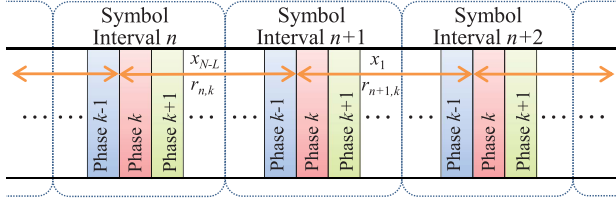
Fig. 2. The signal division for synchronization.

into K phases, as shown in Fig. 2. Let $\boldsymbol{x} = [\boldsymbol{s}, \boldsymbol{d}] = [x_1, \ldots, x_N]$ denote the transmitted signal vector in N successive symbol durations with x_i being the transmitted symbol in the i-th period, $\boldsymbol{s} = [s_1, \ldots, s_L]$ denote the pre-known sync word with $s_i \in \{0, 1\}, 1 \leq i \leq L$, and $\boldsymbol{d} = [d_1, \ldots, d_{N-L}]$ denote the data sequence with $d_j \in \{0, 1\}, 1 \leq j \leq N - L$. Let $r_{i,j}$ denote the number of received photons in the i-th symbol interval starting from phase j. In a photon-counting-based UOWC system, the Poisson model can well characterize the number of received photons during each symbol period. Specifically, assuming the sync word starts from symbol position $n + 1$ and phase k in the received signals, the probability of $r_{n+i,k}$ given the transmitted symbol x_i in the i-th symbol period is [17], [18], [19]

$$\Pr(r_{n+i,k}|x_i) = \frac{(x_i \lambda_s + \lambda_b)^{r_{n+i,k}} e^{-(x_i \lambda_s + \lambda_b)}}{r_{n+i,k}!}, \quad (1)$$

where λ_s and λ_b are signal photon mean and background photon mean, respectively. To facilitate the descriptions, the subscripts i on $r_{i,j}$ will hereafter be taken modulo N, i.e., $r_{i+N,j} = r_{i,j}$.

From (1), the numbers of received photons in the N successive symbol durations can be written in a vector form as

$$\boldsymbol{r}_k = [r_{1,k}, \ldots, r_{N,k}] = \boldsymbol{\alpha} \circ \boldsymbol{x}^{(n)} + \boldsymbol{\beta}, \quad (2)$$

where $\boldsymbol{\alpha} = [\alpha_1, \ldots, \alpha_N]$, α_i denotes the number of signal photons received in the i-th symbol period which follows the Poisson distribution with mean λ_s; $\boldsymbol{\beta} = [\beta_1, \ldots, \beta_N]$, β_i denotes the number of background photons received in the i-th symbol period which follows the Poisson distribution with mean λ_b; "$\circ$" denotes the hadamard product; $\boldsymbol{x}^{(n)} = [x_{N-n+1}, \ldots, x_N, x_1, \ldots, x_{N-n}]$ represents the right circular shift of vector $\boldsymbol{x}$ by n symbol periods, $n \in \{0, \ldots, N-1\}$. Synchronization is to locate the symbol position n and phase k representing the start of sync word based on vector $\boldsymbol{r}_k$.

III. CORRELATION-BASED SYNCHRONIZATION METHOD

A correlation-based synchronization method has been proposed in [12], [20] and [21], which estimates the position of sync word by maximizing the correlation value between the sync word and the number of received photons, i.e.,

$$\left(\hat{n}^c, \hat{k}^c\right) = \arg \max_{n,k} \left[\sum_{i=1}^{L} r_{n+i,k}(2s_i - 1) \right]. \quad (3)$$

After synchronization, the signal photon mean λ_s and background photon mean λ_b can be estimated using the sync word as

$$\hat{\lambda}_b^c = \frac{\sum_{i \in S_0} r_{\hat{n}^c + i, \hat{k}^c}}{|S_0|},$$

$$\hat{\lambda}_s^c = \frac{\sum_{i \in S_1} r_{\hat{n}^c + i, \hat{k}^c}}{|S_1|} - \hat{\lambda}_b^c, \quad (4)$$

where $S_0 = \{i : s_i = 0\}$, $S_1 = \{i : s_i = 1\}$, and "$|\cdot|$" denotes the cardinality of a set.

With the results of synchronization and channel estimation, we can perform symbol detection using the log-likelihood ratio (LLR) criterion as $LLR \gtrless_0^1 0$. According to (1), the LLR is given by

$$LLR = \ln \frac{\Pr(r_{n+i,k}|x_i = 1)}{\Pr(r_{n+i,k}|x_i = 0)}$$

$$= -\lambda_b + r_{n+i,k} \ln \frac{\lambda_s + \lambda_b}{\lambda_b}, \quad (5)$$

where the estimated values are adopted for $(n, k, \lambda_b, \lambda_s)$. Despite the implementation simplicity, the correlation-based method neglects the signals surrounding the sync word and thus leads to a transmission performance degradation. In the following, we propose an improved synchronization method for photon-counting-based UOWC system.

IV. PROPOSED SYNCHRONIZATION METHOD

A. Problem Formulation

We consider joint estimation of sync word position (n, k), signal photon mean λ_s, background photon mean λ_b and data sequence $\boldsymbol{d}$ based on the received vector $\boldsymbol{r}_k$. The joint maximum likelihood (ML) estimation problem is formulated as

$$\left(\hat{n}, \hat{k}, \hat{\lambda}_s, \hat{\lambda}_b, \hat{\boldsymbol{d}}\right) = \arg \max_{n,k,\lambda_s,\lambda_b,\boldsymbol{d}} \Pr\left(\boldsymbol{r}_k|n, k, \lambda_s, \lambda_b, \boldsymbol{d}\right). \quad (6)$$

Under the Poisson distribution given by (1), $\Pr(\boldsymbol{r}_k|n, k, \lambda_s, \lambda_b, \boldsymbol{d})$ can be expressed as

$$\Pr(\boldsymbol{r}_k|n, k, \lambda_s, \lambda_b, \boldsymbol{d})$$

$$= \prod_{i=1}^{L} \frac{(s_i \lambda_s + \lambda_b)^{r_{n+i,k}} e^{-(s_i \lambda_s + \lambda_b)}}{r_{n+i,k}!}$$

$$\cdot \prod_{j=1}^{N-L} \frac{(d_j \lambda_s + \lambda_b)^{r_{L+n+j,k}} e^{-(d_j \lambda_s + \lambda_b)}}{r_{L+n+j,k}!}. \quad (7)$$

Using (7) and taking logarithm, problem (6) can be reformulated as

$$\left(\hat{n}, \hat{k}, \hat{\lambda}_s, \hat{\lambda}_b, \hat{\boldsymbol{d}}\right) = \arg \max_{n,k,\lambda_s,\lambda_b,\boldsymbol{d}} F_1\left(n, k, \lambda_s, \lambda_b, \boldsymbol{d}\right), \quad (8)$$

where

$$F_1(n, k, \lambda_s, \lambda_b, \boldsymbol{d})$$

$$= \sum_{i=1}^{L} \{r_{n+i,k} \ln(s_i\lambda_s + \lambda_b) - (s_i\lambda_s + \lambda_b)\}$$

$$+ \sum_{j=1}^{N-L} \{r_{L+n+j,k} \ln(d_j\lambda_s + \lambda_b) - (d_j\lambda_s + \lambda_b)\}. \quad (9)$$

To reduce the number of jointly estimated unknowns in problem (8), we first maximize $F_1(n, k, \lambda_s, \lambda_b, \boldsymbol{d})$ with respect to $\{\lambda_s, \lambda_b\}$ for given (n, k) and $\boldsymbol{d}$, yielding

$$\hat{\lambda}_b = \frac{\sum_{i=1}^{N} r_{n+i,k} - \left(\sum_{i=1}^{L} s_i r_{n+i,k} + \sum_{j=1}^{N-L} d_j r_{L+n+j,k}\right)}{N - \left(\sum_{i=1}^{L} s_i + \sum_{j=1}^{N-L} d_j\right)},$$

$$\hat{\lambda}_s = \frac{\sum_{i=1}^{L} s_i r_{n+i,k} + \sum_{j=1}^{N-L} d_j r_{L+n+j,k}}{\sum_{i=1}^{L} s_i + \sum_{j=1}^{N-L} d_j} - \hat{\lambda}_b. \quad (10)$$

By substituting (10) into (9), problem (8) can be equivalently transformed into the following problem:

$$\left(\hat{n}, \hat{k}, \hat{\boldsymbol{d}}\right) = \arg \max_{n,k,\boldsymbol{d}} F_2(n, k, \boldsymbol{d}), \quad (11)$$

where

$$F_2(n, k, \boldsymbol{d}) = \sum_{i=1}^{L} r_{n+i,k} \ln\left(s_i\hat{\lambda}_s/\hat{\lambda}_b + 1\right)$$

$$+ \ln\left(\hat{\lambda}_s/\hat{\lambda}_b + 1\right) \sum_{j=1}^{N-L} d_j r_{L+n+j,k}$$

$$+ \ln\left(\hat{\lambda}_b\right) \sum_{i=1}^{N} r_{n+i,k}. \quad (12)$$

Note that exhaustive search for the optimal solution of problem (11) requires high computational complexity. To reduce the complexity, we propose several simplifications to solve problem (11) based on characteristics of data sequence.

B. Simplified Method for Solving Problem (11)

1) Simplification for Symbol Detection: With $d_j \in \{0, 1\}$, the summation $\sum_{j=1}^{N-L} d_j$ equals the number of $d_j = 1$ in $\boldsymbol{d}$, denoted by Δ_d. Given signal photon mean λ_s, background photon mean λ_b and sync word position (n, k) in Poisson channel, the ML detection for data $\boldsymbol{d}$ is equivalent to a threshold-based detection. It implies that $\boldsymbol{d}$ can be determined by detecting the Δ_d largest elements in $\{r_{L+n+1,k}, \ldots, r_{N+n,k}\}$ to be symbol "1" and the remaining elements to be symbol "0". Based on this idea, we sort the signals $\{r_{L+n+1,k}, \ldots, r_{N+n,k}\}$ in descending order such that $\tilde{r}_{n,k}^{(1)} \geq \tilde{r}_{n,k}^{(2)} \geq \cdots \geq \tilde{r}_{n,k}^{(N-L)}$. In the special case
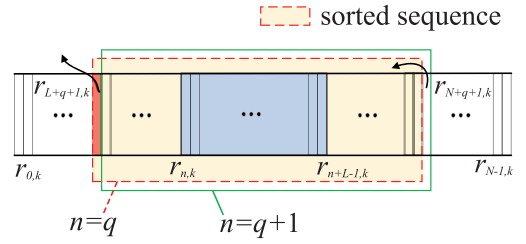

Fig. 3. The simplification of sort operation.

of $\Delta_d = 0$, we set $\tilde{r}_{n,k}^{(0)} = 0$ and $\sum_{j=1}^{N-L} d_j r_{L+n+j,k} = 0$. Then, it yields

$$\sum_{j=1}^{N-L} d_j r_{L+n+j,k} = \sum_{\{j:d_j=1\}} d_j r_{L+n+j,k} = \sum_{j=0}^{\Delta_d} \tilde{r}_{n,k}^{(j)}. \quad (13)$$

By plugging (13) into (12), problem (11) is equivalent to

$$\left(\hat{n}, \hat{k}, \hat{\Delta}_d\right) = \arg \max_{n,k,\Delta_d} F_3(n, k, \Delta_d), \quad (14)$$

where

$$F_3(n, k, \Delta_d)$$

$$= \sum_{i=1}^{L} r_{n+i,k} \ln\left(s_i\hat{\lambda}_s/\hat{\lambda}_b + 1\right)$$

$$+ \ln\left(\hat{\lambda}_s/\hat{\lambda}_b + 1\right) \sum_{j=0}^{\Delta_d} \tilde{r}_{n,k}^{(j)} + \ln\left(\hat{\lambda}_b\right) \sum_{i=1}^{N} r_{n+i,k}. \quad (15)$$

Problem (14) can be solved in three levels: Level i) Under given k, sort the sequence $\mathcal{A}_{n,k} = \{r_{L+n+1,k}, \ldots, r_{N+n,k}\}$ in descending order for each $n \in \{0, \ldots, N-1\}$, yielding the sorted sequence $\mathcal{B}_{n,k} = \{\tilde{r}_{n,k}^{(j)}\}_{j=1}^{N-L}$ with $\tilde{r}_{n,k}^{(1)} \geq \tilde{r}_{n,k}^{(2)} \geq \cdots \geq \tilde{r}_{n,k}^{(N-L)}$. Level ii) For each n, find the optimal Δ_d maximizing $F_3(n, k, \Delta_d)$ in (15), where the maximum value is denoted by $F_3'(n, k)$. Level iii) Find the optimal $n \in \{0, 1, \ldots, N-1\}$ and $k \in \{0, 1, \ldots, K-1\}$ maximizing $F_3'(n, k)$. We can perform simplifications for sorting $\mathcal{A}_{n,k}$ in Level i) and searching Δ_d in Level ii), as presented below.

2) Simplification for Sorting $\mathcal{A}_{n,k}$: Observing $\mathcal{A}_{q+1,k} \cap \mathcal{A}_{q,k} = \{r_{j,k}\}_{j=L+q+2}^{N+q}$, we can further simplify the sort operation in Level i) as n changes from q to $q+1$. Specifically, $\mathcal{A}_{q+1,k}$ can be quickly sorted by deleting $r_{L+q+1,k}$ from $\mathcal{B}_{q,k}$ and then inserting $r_{N+q+1,k}$, in which the former can be readily realized with known position of $r_{L+q+1,k}$ in $\mathcal{B}_{q,k}$ after sorting $\mathcal{A}_{q,k}$, and the latter can be realized through the bisection method. Consequently, the N sort operations for $n \in \{0, \ldots, N-1\}$ can be simplified to single sort operation for $n = 0$, together with the deletion and insertion operations for $n \in \{1, \ldots, N-1\}$. The simplification for sorting $\mathcal{A}_{n,k}$ is illustrated in Fig. 3.

3) Simplification for Searching Δ_d: In Level ii), the search for the optimal $\Delta_d \in \{0, 1, \ldots, N\}$ can be further simplified when n varies form q to $q+1$. Assume the number of $d_j = 1$ in $\boldsymbol{d}$ is Δ_d^q for $n = q$. Since $\mathcal{A}_{q+1,k}$ and $\mathcal{A}_{q,k}$ only differ in the two elements r_{N+q+1} and r_{L+q+1}, Δ_d^{q+1} can only take values

Algorithm 1: The Proposed Synchronization Method.
1:   **Initialization:** Frame length N, sync word length L, sync word $\boldsymbol{s}$.
2:   **for** $k = 0 : K - 1$ **do**
3:     Sort $\mathcal{A}_{0,k} = \{r_{j,k}\}_{j=L+1}^{N}$ in descending order as $\mathcal{B}_{0,k} = \{\tilde{r}_{0,k}^{(j)}\}_{j=1}^{N-L}$ with $\tilde{r}_{0,k}^{(1)} \geq \tilde{r}_{0,k}^{(2)} \geq \cdots \geq \tilde{r}_{0,k}^{(N-L)}$.
4:     $\hat{\Delta}_d^0 = \arg\max_{\Delta_d} F_3(0, k, \Delta_d^0)$.
5:     $F_3'(0, k) = F_3(0, k, \hat{\Delta}_d^0)$.
6:     **for** $n = 1 : N - 1$ **do**
7:     **for** $\Delta_d^n = \hat{\Delta}_d^{n-1} - 1 : \hat{\Delta}_d^{n-1} + 1$ **do**
8:       Calculate $F_3(n, k, \Delta_d^n)$ based on (15).
9:     **end for**
10:     $\hat{\Delta}_d^n = \arg\max_{\Delta_d} F_3(n, k, \Delta_d^n)$.
11:     $F_3'(n, k) = F_3(n, k, \hat{\Delta}_d^n)$.
12:     Delete $r_{L+n+1,k}$ from $\mathcal{B}_{n,k}$.
13:     Insert $r_{N+n+1,k}$ into $\mathcal{B}_{n,k}$ via the bisection method to yield $\mathcal{B}_{n+1,k}$.
14:     **end for**
15:   **end for**
16:   Output $(\hat{n}, \hat{k}) = \arg\max_{n,k} F_3'(n, k)$.

Fig. 4.   The experimental UOWC system.

of $\Delta_d^q - 1, \Delta_d^q$ and $\Delta_d^q + 1$, which greatly reduces the search range for Δ_d^{q+1}.

The overall procedure for solving Problem (14) is summarized in Algorithm 1. Note that the proposed method and correlation method both estimate the sync word position (n, k), where n represents the frame synchronization position and k represents the bit synchronization position. Consequently, these two methods realize both the bit synchronization and frame synchronization simultaneously [12], [20], [21].

C. Complexity Analysis

For the correlation method, the correlation value is calculated $K \times N$ times and each calculation requires a complexity of $O(L)$, so the total complexity is $O(K \times N \times L)$. For the proposed method, the major complexity comes from calculating $F_3(n, k, \Delta_d)$ for each (n, k), which involves a complexity of $O(N)$. Consequently, the total complexity of the proposed method is $O(K \times N^2)$ when n varies from 0 to $N - 1$ and k varies from 0 to $K - 1$.

V. EXPERIMENTAL VERIFICATION

A. Experimental Setup

Fig. 4 shows the experimental photon-counting UOWC system. At the transmitter, a green LED ("Signal-LED", Jred, 520 nm $\sim$ 525 nm) is driven by an arbitrary waveform generator (AWG, Keysight 33612 A) to send the OOK signal with a data rate of 1.25 Mbps, considering the limited bandwidth of the adopted LED and PMT [12], [21], [22]. An optical power meter (Thorlabs PM100D with sensor S130 C) is placed in front of the LED to measure the transmit optical power, which can be adjusted by varying the output voltage of AWG [23], [24], [25]. The total transmit optica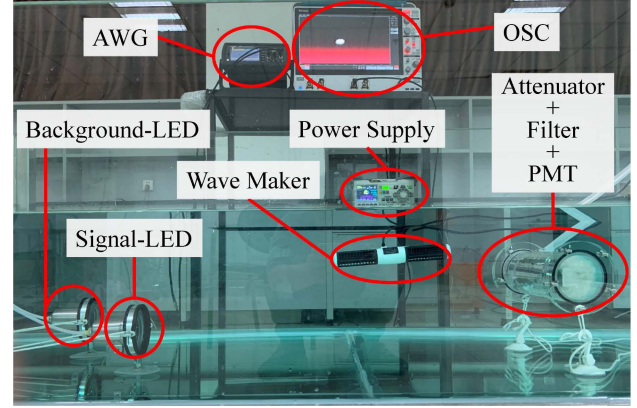l power of LED can be calculated from the measured value by the optical power meter and the ratio of the sensor area to the light spot area. The optical signal propagates through a 0.7-meter UOWC channel. The water in experimental use is clean tap water with an attenuation coefficient about 0.1 m $^{-1}$. The temperature is about 20 °C. A green LED ("Background-LED", Jred, 520 nm $\sim$ 525 nm) is placed near the signal-LED acting as the background light source. At the receiver, a PMT (Hamamatsu CR315) is adopted to detect the number of received photons. To attenuate the optical power and simulate long-distance transmission, an optical attenuator (Thorlabs NE30 A with an optical density of 3.0) is placed in front of the PMT [26], [27], [28]. An optical filter (Smerock FF01-523/20-25) is also employed to filter out the light of other wavelengths. The output of the PMT is recorded by an oscilloscope (OSC, Tektronix MSO64B) with a sampling rate of 250 MSa/s. In order to emulate a dynamic UOWC environment, a wave maker is installed on one side of the water tank. The transmitter and receiver in the water sway with the waves generated by the wave maker, which affects the alignment of the optical link.

In the experiment, a maximum-length sequence of length 31 (i.e., $L = 31$) is chosen as the sync word, and the length of data sequence is set to be $N - L = 400$. The value of K is set to be 200, which is the number of samples during a symbol period. This setting is advantageous for accurate synchronization, as stated in [12], [20] and [21]. To calculate the synchronization error, we adopt an auxiliary signal transmitted through a cable connecting the AWG and OSC as reference signal. This signal helps to provide the exact position (n, k) of the sync word. Then the estimated position $(\hat{n}, \hat{k})$ of the sync word is compared with the exact position (n, k) to obtain a calculated synchronization error as $e = |(\hat{n} - n)K + \hat{k} - k|$. Considering the maximum record length of OSC, we sample 1450 frames at the receiver and obtain the synchronization error of the correlation method and the proposed method. The running time adopting the proposed synchronization method is 8.5 times of that adopting the correlation method, which roughly coincides with complexity analysis in Section IV-C.
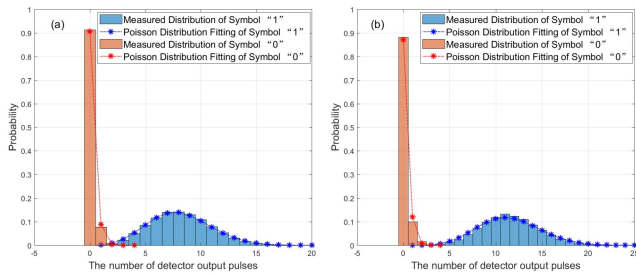
Fig. 5.   Poisson distribution fitting results for the number of detector output pulses under transmit optical power of (a) -1.87 dBm and (b) -0.43 dBm.
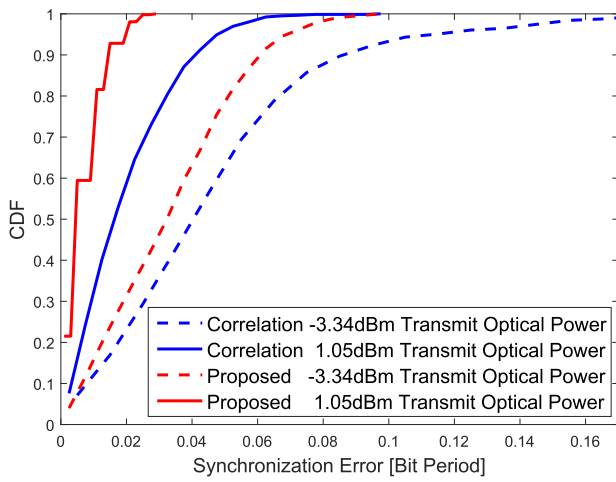

Fig. 6.   The CDF of synchronization error.

TABLE I
THE NUMBER OF FRAME SYNCHRONIZATION ERRORS USING DIFFERENT METHODS

Transmit Optical Power [dBm]	Proposed	Correlation
-4.84	0	13
-3.34	0	5
-1.87	0	0
-0.43	0	0
1.05	0	0
2.47	0	0

Fig. 7.   BER performance under dynamic channel with various signal optical power.

B. Experimental Results

Fig. 5 shows the Poisson distribution fitting results for the number of detector output pulses which is typically used to represent the number of received photons [12], [21], [22]. It is observed that the numbers of pulses in symbol "1" duration and symbol "0" duration both can be well fitted by the Poisson distribution. The fitting results demonstrate the applicability of the Poisson model adopted in this work.

Fig. 6 shows the cumulative distribution function (CDF) of the synchronization error for the correlation method and the proposed method. It is seen that the synchronization performances of both methods improve as the transmit optical power increases. Moreover, compared with the correlation method, the synchronization error of the proposed method is more concentrated around 0, demonstrating the synchronization performance improvement by the proposed method.

Table I lists the number of frame synchronization errors using different methods. It is seen that when the transmit optical power is -4.84 dBm (-3.34 dBm), the correlation method yields 13 (5) frame synchronization errors. In contrast, the proposed method yields no frame synchronization error under all tested transmit optical powers.

Fig. 7 shows the experimental bit error rate (BER) using the correlation method and the proposed method under dynamic channel with various signal optical power. It is observed that the

proposed method can provide an optical power gain exceeding 1 dB over the correlation method. Specifically, at the BER of 10^{-3}, the required optical powers of the correlation method and the proposed method are 0.9 dBm and -0.4 dBm, respectively. Note that the actual running time of the proposed synchronization method can be reduced in several aspects: (1) Adopting parallel computations; (2) Approximating the number of $d_j = 1$ in $\boldsymbol{d}$ as $\Delta_d \approx (N - L)/2$; (3) Properly choosing the length of data sequence in a frame. For instance, in our experiment, the running time of the proposed method can be reduced by 55% using the approximation $\Delta_d \approx (N - L)/2$. As shown in Fig. 7, using the approximation $\Delta_d \approx (N - L)/2$ (labeled as "Suboptimal") can still achieve a noticeable optical power gain over the correlation method.

Fig. 8 shows the experimental BER using the correlation method and the proposed method under dynamic channel with various background optical power. Again, we can see that the proposed method outperforms the correlation method under different background intensities. For the same BER target, the proposed method can tolerate larger background noise than the correlation method.

Note that typical issues in UOWC may include the dispersion, turbulence and misalignment. The above experimental results verify the performance improvement by the proposed synchronization method under the dynamic UOWC environment generated by the wave maker. Such improvement stems from the utilization of the data sequence in a frame in addition
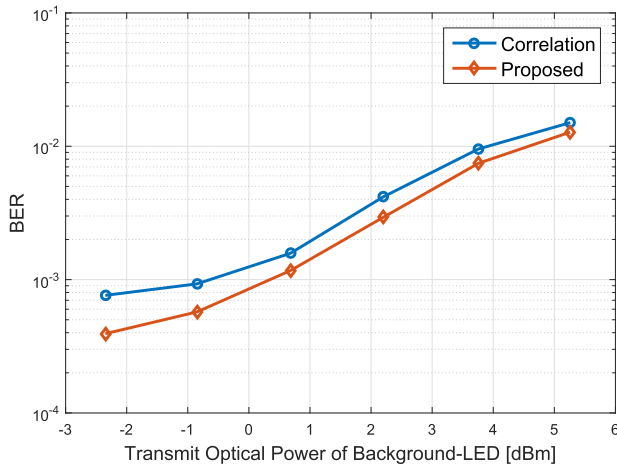
Fig. 8. BER performance under dynamic channel with various background optical power.

to the sync word. Consequently, the proposed synchronization method can be superior to the conventional correlation method in the photon-counting-based UOWC system regardless of the environmental factors.

VI. CONCLUSION

We have proposed an improved synchronization method for the photon-counting-based UOWC system, which jointly estimates the sync word position, signal intensity, background intensity and data sequence based on the received vector in the period of a frame length. Three simplifications have been performed based on the characteristics of data sequence to reduce the complexity for solving the estimation problem. Experimental results have demonstrated the performance superiority of the proposed method over the traditional correlation method.

REFERENCES

[1] J. Xu, "Underwater wireless optical communication: Why, what, and how?," *Chin. Opt. Lett.*, vol. 17, no. 10, Oct. 2019, Art. no. 100007.
[2] Z. Zeng, S. Fu, H. Zhang, Y. Dong, and J. Cheng, "A survey of underwater optical wireless communications," *IEEE Commun. Surv. Tut.*, vol. 19, no. 1, pp. 204–238, Firstquarter 2017.
[3] G. N. Arvanitakis et al., "Gb/s underwater wireless optical communications using series-connected GaN micro-LED arrays," *IEEE Photon. J.*, vol. 12, no. 2, Apr. 2020, Art. no. 7901210.
[4] J. Wang, C. Lu, S. Li, and Z. Xu, "100 m/500 Mbps underwater optical wireless communication using an NRZ-OOK modulated 520 nm laser diode," *Opt. Exp.*, vol. 27, no. 9, pp. 12171–12181, Apr. 2019.
[5] M. Chen, P. Zou, L. Zhang, and N. Chi, "Demonstration of a 2.34 Gbit/s real-time single silicon-substrate blue LED-based underwater VLC system," *IEEE Photon. J.*, vol. 12, no. 1, Feb. 2020, Art. no. 7900211.
[6] K. Kiasaleh, "Delay-and-multiply clock regeneration in APD-based direct-detection optical OOK communication systems," *IEEE Trans. Commun.*, vol. 40, no. 9, pp. 1448–1462, Sep. 1992.
[7] K. Yang, G. Gao, J. Ning, J. Zhang, and H. Peng, "High speed underwater wireless optical communication with high receiver sensitivity and large dynamic range," in *Proc. 9th Int. Conf. Inf., Commun. Netw.*, 2021, pp. 220–224.

[8] Y. Cheng et al., "50 m/187.5 Mbit/s real-time underwater wireless optical communication based on optical superimposition," *Chin. Opt. Lett.*, vol. 21, no. 2, Feb. 2023, Art. no. 020601.
[9] J. Ning, G. Gao, J. Zhang, H. Peng, and Y. Guo, "Adaptive receiver control for reliable high-speed underwater wireless optical communication with photomultiplier tube receiver," *IEEE Photon. J.*, vol. 13, no. 4, Aug. 2021, Art no. 7300107.
[10] C. Gong and Z. Xu, "Channel estimation and signal detection for optical wireless scattering communication with inter-symbol interference," *IEEE Trans. Wireless Commun.*, vol. 14, no. 10, pp. 5326–5337, Oct. 2015.
[11] A. A. D'Amico, G. Colavolpe, T. Foggi, and M. Morelli, "Timing synchronization and channel estimation in free-space optical OOK communication systems," *IEEE Trans. Commun.*, vol. 70, no. 3, pp. 1901–1912, Mar. 2022.
[12] X. Liu, C. Gong, S. Li, and Z. Xu, "Signal characterization and receiver design for visible light communication under weak illuminance," *IEEE Commun. Lett.*, vol. 20, no. 7, pp. 1349–1352, Jul. 2016.
[13] E. Zedini, H. M. Oubei, A. Kammoun, M. Hamdi, B. S. Ooi, and M.-S. Alouini, "Unified statistical channel model for turbulence-induced fading in underwater wireless optical communication systems," *IEEE Trans. Commun.*, vol. 67, no. 4, pp. 2893–2907, Apr. 2019.
[14] J. Massey, "Optimum frame synchronization," *IEEE Trans. Commun.*, vol. 20, no. 2, pp. 115–119, Apr. 1972.
[15] A. R. Hammons and F. Davidson, "Near-optimal frame synchronization for free-space optical packet communications," in *Proc. IEEE Mil. Commun. Conf.*, 2010, pp. 797–801.
[16] G. Lui and H. Tan, "Frame synchronization for direct-detection optical communication systems," *IEEE Trans. Commun.*, vol. 34, no. 3, pp. 227–237, Mar. 1986.
[17] J. Li, D. Ye, K. Fu, L. Wang, J. Piao, and Y. Wang, "Single-photon detection for MIMO underwater wireless optical communication enabled by arrayed LEDs and SiPMs," *Opt. Exp.*, vol. 29, no. 16, pp. 25922–25944, Aug. 2021.
[18] J. Li et al., "Photon-counting schemes for MIMO underwater wireless optical communication with arrayed PMTs," *Appl. Opt.*, vol. 61, no. 2, pp. 403–409, Jan. 2022.
[19] Y. Zhu, C. Gong, Y. Ding, and Z. Xu, "Weak signal detection for visible light communication in the pulse and transition regimes of an operational PMT detector via an SVM-based learning method," *Opt. Exp.*, vol. 30, no. 8, pp. 12456–12473, Apr. 2022.
[20] C. Wang, H.-Y. Yu, Y.-J. Zhu, T. Wang, and Y.-W. Ji, "Experimental study on SPAD-based VLC systems with an LED status indicator," *Opt. Exp.*, vol. 25, no. 23, pp. 28783–28793, Nov. 2017.
[21] G. Wang, K. Wang, C. Gong, D. Zou, Z. Jiang, and Z. Xu, "A 1 Mbps real-time NLOS UV scattering communication system with receiver diversity over 1 km," *IEEE Photon. J.*, vol. 10, no. 2, Apr. 2018, Art no. 7903013.
[22] D. Zou, C. Gong, K. Wang, and Z. Xu, "Characterization on practical photon counting receiver in optical scattering communication," *IEEE Trans. Commun.*, vol. 67, no. 3, pp. 2203–2217, Mar. 2019.
[23] Y. Huang, Z. Guo, X. Wang, H. Li, and D. Xiang, "GaN-based high-response frequency and high-optical power matrix micro-LED for visible light communication," *IEEE Electron Device Lett.*, vol. 41, no. 10, pp. 1536–1539, Oct. 2020.
[24] Y.-C. Chung, H.-H. Chung, and S.-H. Lin, "Improvement of temperature and optical power of an LED by using microfluidic circulating system of graphene solution," *Nanomaterials*, vol. 11, no. 7, Jun. 2021, Art. no. 1719.
[25] H. O. Durmuş, E. Ç. Arı, B. Karaböce, and M. Y. Seyidov, "Experimental evaluation of temperature and optical power generated by a LED therapy device on an agar phantom," in *Proc. IEEE Int. Symp. Med. Meas. Appl.*, 2022, pp. 1–6.
[26] H. Chen et al., "Toward long-distance underwater wireless optical communication based on a high-sensitivity single photon avalanche diode," *IEEE Photon. J.*, vol. 12, no. 3, Jun. 2020, Art no. 7902510.
[27] X. Sun et al., "Non-line-of-sight methodology for high-speed wireless optical communication in highly turbid water," *Opt. Commun.*, vol. 461, Jan. 2020, Art. no. 125264.
[28] X. Chen et al., "Computational temporal ghost imaging for long-distance underwater wireless optical communication," *Opt. Lett.*, vol. 46, no. 8, pp. 1938–1941, Apr. 2021.